Bone remodeling in a new biomimetic polymer-composite hip stem

Bougherara, Habiba; Bureau, Martin N.; Yahia, L'Hocine

Publisher's version / Version de l'éditeur:
https://doi.org/10.1002/jbm.a.32346
Journal of Biomedical Materials Research Part A, 92A, 1, pp. 164-174, 2009-01

Journal of Biomedical
Materials Research
Part A

Bone remodeling in a new biomimetic polymer-composite hip stem

Journal:	*Journal of Biomedical Materials Research: Part A*
Manuscript ID:	JBMR-A-06-0855.R1
Wiley - Manuscript type:	Original Article
Date Submitted by the Author:	n/a
Complete List of Authors:	Bougherara, Habiba; Laboratory for Innovation and Analysis of Bioperformance, ©cole Polytechnique de Mont©al, G©nie Biom©dical Bureau, Martin; National Research Council Canada, Industrial Materials institute, Functional Polymer Systems Yahia, L'Hocine; ©cole Polytechnique de Mont©al, G©nie biom©dical
Keywords:	Biomimetic composite hip stem, Adaptive bone remodeling, Stress shielding, Strain energy density, Finite Element Method

Bone remodeling in biomimetic polymer-composite hip stem prosthesis

Habiba Bougherara[1*], Martin N Bureau[2], L'Hocine Yahia[1]

[1] Laboratory for Innovation and Analysis of Bioperformance, École Polytechnique, Montréal, Québec, Canada, H3T 1J4
[2] Functional Polymer Systems, Industrial Materials Institute, National Research Council Canada Boucherville, Québec, Canada, J4B 6Y4

Key words: Biomimetic hip composite stem, Internal bone remodeling, Strain energy density, Total hip replacement, Finite element method.

Presented to

Journal of Biomedical Materials Research Part A

Revised version

May 18, 2007

* Corresponding author: Dr. Martin Bureau, Tel: 450-641-5179, Fax : 450-641-5105; martin.bureau@cnrc-nrc.gc.ca .

Bone remodeling in a new biomimetic polymer-composite hip stem

ABSTRACT

Adaptive bone remodeling is an important factor that leads to bone resorption in the surrounding femoral bone and implant loosening. Taking into account this factor in the design of hip implants is of clinical importance, since it allows the prediction of the bone-density redistribution and enables the monitoring of bone adaptation after prosthetic implantation. In this paper adaptive bone remodeling around a new biomimetic polymer-composite based (CF/PA12) hip prosthesis is investigated in order to evaluate the amount of stress shielding and bone resorption. The design concept of this new prosthesis is based on a hollow sub-structure made of hydroxyapatite-coated, continuous carbon fiber (CF) reinforced polyamide 12 (PA12) composite with an internal soft polymer-based core. Strain energy density theory coupled with 3-D Finite Element models are used to predict bone density redistributions in the femoral bone before and after total hip replacement using both polymer-composite and titanium stems. The result of numerical simulations of bone remodeling revealed that the CF/PA12 composite stem generates an excellent bone density pattern compared to the titanium-based stem, indicating the effectiveness of the composite stem to reduce bone resorption caused by stress shielding phenomenon. This may result in an extended lifetime of Total Hip Replacement (THR).

INTRODUCTION

The most common reason for failure of total hip replacement (THR) surgery is aseptic loosening.[1,2] This problem occurs as a result of several mechanisms including osteolysis induced by wear debris, bone resorption caused by stress shielding and migration due to large micromotions at the implant-tissue interface. Aseptic loosening tends to be painful, and usually requires revision hip replacement. When compared with primary THR, revision surgeries are more complicated and the outcomes are less satisfactory.

Although success has been consistently achieved with most THR's over the last 40 years[3], factors related to implant longevity and a younger, more active population of patients have led to a significant increase in the absolute number of failed THR's. A recent projection study showed that the number of THR revisions will increase 137% from 2005 to 2030 in the US[4]. Therefore, the need to improve the survivability of hip implants, *i.e.,* reducing the rate of THR revisions, will be one of the orthopedic challenges for the next decades.

Bone is a living tissue and, like most living organisms, needs continuous adaptation to maintain its architecture. The regulation of bone structure, as well as its adaptation in response to different load conditions, is controlled by the mechanism of bone remodeling. After implantation, femoral periprosthetic bone experiences resorptive bone remodeling caused by the alteration of the stress-strain, *i.e.,* stress shielding.[5,6] Resorptive bone

remodeling may cause inadequate bone stock maintenance, leading to aseptic loosening and implant failure[7]. It will also complicate THR revision eventually.

The process of bone remodeling has attracted the focus of researchers ever since the law of bone functional adaptation postulated by Wolff in the 19th century. Several experimental studies and computational models have been developed to understand the relationship between the mechanical loading and the functional adaptation of bone; see for instance, Cowin and Hegedus,[8] Carter and Hayes,[9] Cowin et al.,[10] Beaupré et al.,[11] Prendergast and Taylor,[12] Levenston and Carter[13] and Wang and Dumas[14]. More specific studies[15-18] have successfully applied different bone remodeling theories to estimate the outcome of bone remodeling after conventional total hip surgery.

Nowadays, conventional implants still undergo problems of biomechanical mismatch of elastic modulus and interfacial stability with host tissues. Fortunately, fiber-reinforced polymer composites provide an interesting solution to face these problems since they have excellent mechanical properties, such as high fatigue and creep resistance, rigidity and stiffness. Moreover, these materials have rapid, versatile and inexpensive fabrication processes.

The feasibility of the proposed biomimetic polymer-composite prosthesis previously described by Campbell et al.[19] and Bougherara et al.[20] was evaluated and validated numerically and experimentally. Preliminary tests investigating the biocompatibility of the biomimetic composite stem showed that the composite produced no adverse cytotoxic

response in the peri-prosthetic tissues[21], and tests using simulated body fluid conditioning showed that the hydroxyapatite (HA) coated composite has excellent potential of biocompatibility.[22]

A key feature of this new biomimetic composite stem is this proximal HA coating that will allow stable short and long-term fixation of prosthesis with minimal bone loss through stress shielding. This new biomimetic composite stem differs significantly from the previous design of lower stiffness composite femoral stems that consisted of a fairly rigid core with low modulus fixation surface[23-26]. It was shown that this surface was prone to high shear deformation and resulted in poor bone fixation and formation of fibrous tissues. Early failure of these femoral stems (*i.e.*, isoelastic) were related to a lack of fixation, which caused loosening.[27]

This new biomimetic composite stem is also quite different from the recently studied cobalt-chrome (Co-Cr) stem with a surface layer of polyaryletherketone (PAEK) and a fully porous titanium (Ti) mesh coating[28-32], which clinically showed the expected reduced bone loss, and stable initial and mid-term bone fixation. The overall stiffness of this stem, calculated from the bending stiffness[28] is however still higher than that of cortical bone's.

Following the literature, all bone remodeling simulations are conducted on conventional metallic implants (*e.g.*, titanium, cobalt-chrome and stainless steel alloys). However, no single numerical study has been reported for investigating bone remodeling when HA-

coated composite prostheses are implanted. Therefore, further work is needed in this area. The aims of this study are thus: 1) to simulate the bone remodeling process in the proximal femur around a new biomimetic composite hip prosthesis using strain energy density model combined with Finite Element Method (FEM); and 2) to compare bone density distributions after THR using the composite-based hip and titanium alloy-based (Ti-6Al-4V) stems.

MATERIALS AND METHODS

Model of bone remodeling

The bone remodeling model adopted in this paper is based on the one developed by Huiskes et al.[16] and expanded later by Weinans et al.,[33] incorporating the dead zone concept. This model uses strain energy density (*SED*) or U as the mechanical signal that launches and controls the bone remodeling process. The strain energy density U can be expressed as function of stresses and strains by the following equation:

$$U = \frac{1}{2}\sigma_{ij}\varepsilon_{ij} \tag{1}$$

The internal bone remodeling theory assumed that the relation between the strain energy density and the rate of change of bone density is linear. The remodeling governing equation can be written as follows:

$$\frac{d\rho}{dt} = B(U-k), \quad 0 < \rho \le \rho_{cb} \tag{2}$$

where ρ represents the apparent density of the bone, ρ_{cb} is the maximum density of the cortical bone, the constants B and k represent the remodeling rate and the site-specific reference strain energy density respectively.

Carter et al.[34] have shown that bone remodeling will not occur if there is no difference between the actual strain energy density (*SED*) and site-specific reference (target) one (k). This difference known as stimuli (S) is the driving force for adaptation process. In other words, there are thresholds to be exceeded before bone adaptation could occur. The zone, where no adaptive response occurs ($2s$) is called 'dead zone' (Fig. 1).

Considering the concept of the dead zone, the new equations for internal bone remodeling are reformulated as follows:

$$\frac{d\rho}{dt} = \begin{cases} B\left[U-(1-s)k\right], & \text{if } U \le (1-s)k \quad \text{resorption,} \\ 0, \text{ if } (1-s)k < U < (1+s)k & \text{dead zone,} \\ B\left[U-(1+s)k\right], & \text{if } U \ge (1+s)k, \text{ formation} \end{cases} \tag{3}$$

The differential equation of bone remodeling (Eq. 3) is solved using Euler's forward method with a constant time step Δt. The change in bone density $\Delta\rho(x)$ in each step is obtained by the following expression:

$$\begin{aligned} &\Delta\rho(x) = \Delta t.\left(\frac{d\rho}{dt}\right) \\ &0 < \rho \le \rho_{cb} \end{aligned} \tag{4}$$

The new bone density in each element is then calculated by the following equation:

$$\rho(x,t+\Delta t) = \rho(x,t) + \Delta\rho(x,t) \tag{5}$$

Convergence of this iterative process is considered when no significant changes in density of elements are observed (*i.e.* current density minus density at prior time step tends to zero) or when the bone density has reached its maximum or minimal values. In order to make sure that convergence of remodeling process is reached, the following convergence criterion for density is used:

$$CONVD = \frac{1}{n}\sum_{i=1}^{n}\left|\left(\rho_i^{(t)} - \rho_i^{(t-1)}\right)\right| \tag{6}$$

where n is the number of elements in the FEM, *CONVD* is the sum of the mean absolute values of variation in relative apparent density.

The value of *CONVD* is calculated after each iteration, when no further change in density is observed (*i.e., CONVD* approaches to zero) bone remodeling equilibrium is reached. Weinans et al.[33] noticed that the remodeling objective $U = k$ will not be met in elements in which the bone resorbs completely ($\rho = 0.01$) or in which cortical bone is obtained ($\rho = \rho_{cb}$), the remodeling process stops; hence, the remodeling objective $U = k$ will not be met.

The boundary condition for the predicted apparent density is given by:

$$\rho_{\min} < \rho < \rho_{cb} \tag{7}$$

The elastic modulus is determined by the empirical relationship under compressive loading proposed by Carter and Hayes,[9] in which the bone density (g/cm^3) is correlated to the elastic modulus (MPa) as follows:

$$E = a\rho^3 \tag{8}$$

where a is constant.

Sensitivity analyses for two different density modulus relationships were conducted by Weinnans et al.[35] The first relationship taken from Carter and Hayes[9] and the second relationship taken from Goldstein et al[36]. Results showed that the FE models provide consistent stress-shielding patterns in the bone, independent of the choice of the bone density modulus relationship used in the computer model.

For the numerical simulation of the femoral model, Weinans et al.[33] used the values of constant parameters presented in Table 1. The authors showed that these parameter values produced density distribution that was similar to the one obtained by Fyhrie and Carter,[37] indicating some resemblance to the natural distribution in the femur. Also, a comparison between animal experiments and adaptive remodeling simulation around bonded non-cemented THR showed similar amounts of proximal bone loss and distal bone densification.[15]

In the present simulation parameter values in Table 1 are considered since they lead to realistic bone configuration. Values of the remaining parameters, *i.e.,* values of the starting bone density ρ_0 and the time step Δt, are chosen so that they provide realistic bone density distributions and ensure the stability of the iterative process $\left(\Delta t = 20 \text{ time unit}, \rho_0 = 0.8 \ \left(\text{g/cm}^3\right)\right)$.

3-D geometries of the proximal femur and the prosthesis

Computerized tomography (CT) scan sections of the composite femur were used to generate the 3-D geometric model of the proximal femur[38] (Fig. 2). The bone material was assumed to be isotropic and linear-elastic. The initial value of bone density was considered homogenous in the whole bone volume and was set to 0.8 g/cm^3. The material properties of the bone in the first time step depended on the initial value of bone density; in the next time steps the properties changed with bone density change. According to Balle[39], Kuhl and Balle[17], a number of case studies has shown that the initial bone density does not have a significant influence on the final density distribution. The initial Young modulus corresponded to the initial bone density was calculated from Eq. 8 to be 1940 MPa, with a equal to 3790 and initial bone density ρ of 0.8 g/cm^3. Poisson's ratio ν was assumed to be equal to 0.3.

The 3-D geometry of the modular composite hip stem prosthesis is shown in Figure 3a. This stem is straight, follows the antecurvation of the shaft of the femoral bone, has an oval cross-section, and a shaft angle of 135°. The solid model of the prosthesis was created using commercially available software (CATIAV5R13; Dassault Systèmes, Montreal, CA). The design concept of the biomimetic stem is inspired from the structure of the femoral bone itself.[40] The latter is made of a polymer composite material with a variable density close to that of the cortical bone (density ranged of between 1.6 and 2.1 g/cm^3) to close to that of the spongy bone (density of between 0.03 and 0.12 g/cm^3).[40] It is composed of 3 mm sub-structure thickness composite of a carbon fiber

(CF)/polyamide 12 (PA12) with carbon fiber content of 68%, as determined from thermal gravimetric analysis (TGA), a 100 microns thick bioactive HA coating in the proximal section and an internal polymeric core. The bioactive HA coating was introduced to promote bone osteointegration and enhance the fixation strength. The sub-structure of the stem is composed of concentric layers of braided commingled composite fibers with pre-determined fiber orientation to reproduce the stiffness of the cortical bone (elastic modulus to be between 12 and 20 GPa).[40,41] This particular braiding architecture combines filament winding and weaving. The fiber orientation or the helix angle varied between 20° and 50°. 40 spindles of thread were mounted on the carriers in order to obtain a thread-to-thread weave pattern. In the FEM study, an approximate fiber orientation of ±45° for the braided layers was considered (see Fig. 3b). For the polymeric core, typical values of different polyethylene grades (low density or high density) were considered. The values of the elastic properties used for the composite material are shown in Table 2.[19]

Details of the FE models, boundary and load conditions

Three dimensional finite element models are constructed and analyzed using the software (ANSYS 10.0; Ansys, Inc., Montreal, CA). The first model represents the intact femoral bone (Fig. 4a), the second and the third ones represent THR using conventional Ti-base alloy (E = 110 GPa, ν = 0.3) and biomimetic composite (CF/PA12) stems respectively. The bone-implant interface is modeled using surface-to-surface contact elements (CONTA174 and TARGE170). For the two THR models, the interface condition between

the proximal prosthesis surface (HA surface) and cancellous bone as well between distal prosthesis and cortical bone was modeled by contact elements (CONTAC174 – 8 nodes with dynamic friction capabilities). Two values of the friction coefficient were used: 1.0 at the bone-HA interface and 0.6 throughout the stem surface simulating stick/slip friction behavior. Fully-bonded conditions were assumed at all other interfaces in view of interfacial adhesion measured from pull tests.[22]

The FE composite model was made of two types of elements: 3-D structural solid elements (SOLID45-8 nodded tetrahedral element with three degrees of freedom at each node) are used to simulate the femoral bone and the internal core. SOLID45 element is usually used for the 3-D modeling of solid structures with plasticity, creep, stress stiffening, large deflection, and large strain capabilities. Multi-layer linear structural shell elements (Shell99-8 nodded quadratic element with six degrees freedom at each node) are employed to simulate the composite sub-structure. Generally SHELL99 element is used for layered applications of a structural shell model and allows up to 250 layers. Each layer of the shell element has two variables: thickness and direction angle.

The complete FE composite model consisted of 8497 nodes, 25993 elements and 10247 contact elements.

Each FE model is loaded the most critical load case of gait (a single limb stance phase) and consisted of a 3.41 kN force applied to the femoral head and a 2.59 kN abductor

muscle forces. Additionally, two frequent activities mainly walking and stair climbing were considered to address the effect of loading condition on bone density distribution.

The magnitudes and directions of these loads, resolved along each of the anatomic directions, are as given in the literature[42,43] (see Table 3 and 4). The loads were distributed over several nodes to avoid stress concentration and the displacement of all nodes at the distal end of the femoral bone is rigidly constrained.

RESULTS

Convergence of bone remodeling process

A numerical code was generated in ANSYS macros to solve bone remodeling process described by Eq. 3. This process starts from a constant bone density of 0.8 g/cm^3 and ends with variable density distributions at the equilibrium condition.

The convergence criterion (Eq. 6) of the iterative process is plotted in Figure 5. This figure illustrates the variation of the mean change in bone density per number of elements versus the number of iterations (N). It is clearly seen from this figures that the convergence of the calculated results is obtained when N reaches 60 iterations.

Bone density distribution in the FE models

The mean bone density distributions in the three FE models employed, computed using $N = 60$, are presented in Figures 6 and 7 (3D and section views). In the calcar region

(zone below the neck resection or Gruen zone seven), the mean values of bone density range between 1.0 and 1.7 g/cm^3 for the intact femoral bone, while in the distal part of the femur these values range between 1.4 and 1.74 g/cm^3. When the Ti stem is used, the mean values of bone density in Gruen zone seven range between 0.01 and 0.9 g/cm^3, whereas the composite stem generates bone density between 0.8 to 1.7 g/cm^3. These values show up to 40% reduction in bone density when the conventional implant is used. However, in Gruen zone four (region around the distal tip of the implant), bone density distributions are quite similar for both Ti and CF/PA 12 stems as can be seen from Figure 8. In the remaining zones (*i.e.* zone 1, 2, 3, 5, 6), values of bone density are lower for the titanium stem than those found with CF/PA 12 stem by approximately 20 to 30%.

These results are confirmed by FEM analyses of cross sections (sliced views) of the proximal femoral bone in Figures 8 and 9. By comparing the density distribution in the intact femoral bone with the one implanted with CF/PA12 composite stem (Figs. 8b and 9b), it appears that the bone density distributions are quite close to each other, indicating the potential of the composite stem to reduce stress shielding and bone resorption.[5] On the contrary, bone density distributions using Ti stem are lower than those found in the intact femoral showing that stiff materials lead to bone resorption.

Strain energy distribution in the FE models

It is obvious that the strain energy (SE), as well as the strain energy density (SED) decrease after total hip replacement. Figures 10 and 11 illustrate the strain energy density for the three FE models used in this study. The mean values of the strain energy density

in natural femur vary from 0.24 to 5.3 mJ/cm^3. These values range between 0.21 and 4.3 mJ/cm^3 for the composite stem, and between 0.07 and 3.7 mJ/cm^3 for Ti stem. As can be seen from these figures, strain energy density patterns (Figs 10a and 11a) in the intact femoral bone are higher than those found in the femoral bone implanted with both prostheses (Figs 10b, 10c, 11b and 11c). Peak SED in the intact femur is approximately 18 % and 30% higher than that using the CF/PA 12 and Ti stems respectively. However, the composite stem exhibits higher strain energy density distribution (Fig. 10b) in the proximal part of the femur (especially in the calcar region) than the stem made of titanium alloys.

Influence of loading conditions on stress shielding using the composite stem

The effect of load variation on bone resorption and stress shielding using the composite stem was evaluated by calculating the bone density distribution for two activities, walking and stair climbing (see Figure 12 and 13). The density patterns for both activities are quite similar, however, walking load generates a slightly higher bone density, i.e., reduced stress shielding, in the proximal part of the femur than stair climbing loading. This is due to the joint force magnitude in the vertical direction (z) 35% greater for walking than stair climbing. On the contrary, in the mid and distal region, the resulting density is lower for walking. For this load case, lower load is transferred to this region because the magnitude of circumferential joint force component (in the y direction) is 27% less than the one in stair climbing.

DISCUSSION

Many research have demonstrated that analytical and numerical models may be used before conducting extensive experimental tests as initial tools to evaluate components for the design of composite hip implants.[45,46] Bone remodeling after THR was simulated to assess the amount of stress shielding in the new biomimetic composite stem. The bone remodeling theory based on strain energy density used for this study to demonstrate the potential of the biomimetic composite stem was tested experimentally in five elderly patients[47]. Investigation of bone density using dual energy X-ray absorptiometry (DEXA) showed that the predicted bone loss agree nicely with the DEXA measurements on the retrievals.

In this study, two surgical procedures were evaluated and compared to the initial bone configuration. The first one was the THR with conventional biomedical Ti-6Al-4V and the second one used a new biomimetic composite stem. Three FE models were employed to compute the strain energy and bone density distribution. Results of numerical simulations have shown that the biomimetic composite prosthesis results in bone density closer to that obtained in the intact femoral bone when compared to Ti-6Al-4V stems. This is consistent with previous work conducted on flexible composite and metallic femoral components.[48] In addition, the biomimetic stem generates considerably higher bone density and strain energy density than the Ti-6Al-4V prosthesis in the proximal part of the femur, due to its resulting stiffness closer to that in the intact femoral bone. Unlike

the composite stem, Ti-6Al-4V stem leads to severe bone resorption in the proximal part of the femur, in agreement with other studies.[15,49] It can be explained by the fact that the Ti alloy-based prosthesis, which have a high stiffness (110 GPa), sustains the greater part of the load and transmits it to the distal part of the femoral bone. This is consistent with previous stress analyses that were performed by[50-52] on fiber-reinforced polyetheretherketone composite (CF/PEEK).

Results of numerical simulations have also shown that loading conditions have a slight effect on stress shielding along the entire length of the composite hip implant. Stress shielding in the calcar region is dominated by the vertical component of the joint force,[53] while it is dominated by the circumferential component of the joint force in the distal part.

In the present study, the finite element models, as well as the mathematical model used for bone remodeling included many hypotheses and simplifications, which may influence interpretation of results. First, for the FEM, all muscles forces are assumed inactive accept abductors. Considering other muscle actions (*e.g.*, iliotibial tract muscle) affects the stress distribution, which in turn, may influence SED and bone density distributions[35]. Second, the mathematical model of bone remodeling (Eq. 3) does not include the external remodeling, including the reshaping of the cortical surfaces. However, it is well-known that after hip arthroplasty, changes occur in the geometry of the bone and, consequently, these changes may influence the results. Furthermore, the time step involved in the

iterative procedure for the prediction of bone density is not related to physical (real) time step.

Even though adaptive bone remodeling model based on strain energy includes some limitations, this remodeling model can provide valuable information on stress shielding and bone resorption, which are important factors that should be taken into account for the design of any new implant. A possible extension of the present work would be to consider a more realistic model of bone adaptation, which takes into account the biological and biochemical processes. A new thermodynamic model based on irreversible thermodynamics and kinetics of chemical reactions has been recently developed by our group.[54] We believe that this new model is a powerful tool to design implants. It can be also used to predict and provide treatment of several diseases connected with bone remodelling such as osteoporosis. Therefore the application of this thermodynamic bone remodeling model may reach the clinically broad domain.

CONCLUSION

Prediction of bone remodeling based on strain energy around HA-coated composite hip stems showed that the biomimetic based-composite stem, which have stiffness close to that in the intact femoral bone, produces between 20 and 40% more bone density in the proximal femur and quite similar bone density in the distal part than the conventional metallic stems. This indicates the benefits of the composite-based biomimetic stem design in reducing bone resorption and fracture risk. In addition, this investigation showed that load conditions have a slight effect on stress shielding.

ACKNOWLEDGMENTS

This project is supported by Natural Sciences and Engineering Research Council of Canada (NSERC) and Terray Corporation. Special thanks to Dr. Johanne Denault and Dr. Jean-Gabriel Legoux from the Industrial Materials Institute of the National Research Council Canada (NRC). The technical support of Navid Arjmand from École Polytechnique of Montreal is gratefully acknowledged.

FIGURE LEGENDS

Figure 1: Bone remodeling process as described by Huiskes et al.[16]

Figure 2: Three dimensional geometry of the femoral bone: a) intact bone and b) cut bone.

Figure 3: Biomimetic hip stem and coordinate system: a) concept design and b) 3-D geometry of the composite stem. Ply configurations used for the composite material [$(\pm 45°)_6$].

Figure 4: 3-D FE models: a) intact femoral bone, b) femoral bone with CF/PA12 stem and c) femoral bone with Ti stem.

Figure 5: Variation of mean change in density (CONVD) versus the number of iterations (N).

Figure 6: 3D view of bone density distribution (g/cm^3): a) intact femur, b) with CF/PA12 stem and c) with Ti stem.

Figure 7: Section view of bone density distribution (g/cm^3): a) intact femur, b) with CF/PA12 stem and c) with Ti stem.

Figure 8: A slice view trough the vertical axe of the femur: a) intact femur, b) with CF/PA12 stem and c) with Ti stem.

Figure 9: a) A slice through the proximal section of the femur, b) bone density distributions in the cross section (A-A)

Figure 11: Strain energy density distribution (Joule/cm^3): a) intact femur, b) with CF/PA12 stem and c) with Ti stem

Figure 12: Effect of load variation on bone density distribution (g/cm^3) using: a) walking load and b) stair climbing load

Figure 13: A slice view of bone density in the proximal femur (g/cm^3) using: a) walking load and b) stair climbing load

REFERENCES

1. Buford A, Goswami, T. Review of wear mechanisms in hip implants: Paper I - General. Materials & Design 2004;25(5):385-393.
2. Sargeant A, Goswami, T. Hip implants: Paper V. Physiological effects. Materials & Design 2006;27(4):287-307.
3. Berry D, Harmsen WS, Cabanela ME, Morrey B F Twenty-five-year survivorship of two thousand consecutive primary charnley total hip replacements : Factors affecting survivorship of acetabular and femoral components. J. Bone Joint Surg. Am. 2002;84(2):171 - 177.
4. Kurtz S, Lau E, Zhao K, Mowat F, Ong K, Halpern K. The future burden of hip and knee revisions: U.S. Projections from 2005 to 2030. 2006; Chicago, US.
5. Huiskes R, Weinans H, Rietbergen BV. The relationship between stress shielding and bone resorption around total hip stems and effects of flexible materials. Clinical Orthopaedic and Related Research 1992;274:124-134.
6. Lengsfeld M, Burchard R, Gunther D, Pressel T, Schmitt J, Leppek R, Griss P. Femoral strain changes after total hip arthroplasty —patient-specific finite element analyses 12 years after operation. Medical Engineering & Physics 2005;27(8):649-654.
7. Bougherara H, Bureau MN, Campbell M, Vadean A, Yahia L'H Design of a biomimetic polymer-composite hip prosthesis. J. Biomed. Mater. res. 2006;(in press).
8. Cowin S, Hegedus DH. Bone remodeling I: Theory of adaptive elasticity. J. Elasticity 1976;6(3):313-326.
9. Carter D, Hayes WC. The behavior of bone as a two-phase porous structure. J. Bone Joint Surg. 1977;59(A):954-62.
10. Cowin S, Hart RT, Balser JR, Kohn DH. Functional adaptation in long bones: establishing in vivo values for surface remodeling rate coefficients. J. Biomechanics 1985;18:665-84.
11. Beaupre G, Orr TE, Carter DR. An approach for time-dependent bone modeling and remodeling-application: a preliminary remodeling simulation. J. Orthop. Res. 1990;8(5):662-70.
12. Prendergast P, Taylor D. Prediction of bone adaptation using damage accumulation. J. Biomechanics 1994;27:1067-76.
13. Levenston M, Carter DR. An energy dissipation-based model for damage stimulated bone adaptation. Journal of Biomechanics 1998;31(7):579-586.
14. Wang X, Dumas GA. Simulation of bone adaptive remodeling using a stochastic process as loading history. Journal of Biomechanics 2002;35(3):375-380.
15. Weinans H, Huiskes R, Van Rietbergen B, Sumner DR, Turner TM, Galante JO. Adaptive bone remodeling around bonded noncemented total hip arthroplasty: A comparison between animal experiments and computer simulation. Journal of Orthopaedic Research 1993;11(4):500-513.
16. Huiskes R, Weinans H, Grootenboer HJ, Dalstra M, Fudala B, Slooff TJ. Adaptive bone-remodeling theory applied to prosthetic-design analysis. J. Biomechanics 1987;20:1135-50.

17. Kuhl E, Balle F. Computaional modeling of hip replacement surgery: total hip replacement vs. hip resurfacing. Technische Mecanik; 2005. p 107-114.
18. Pawlikowski M, Skalski K, Haraburda M. Process of hip joint prosthesis design including bone remodeling phenomenon. Computers and Structures 2003;81:887-893.
19. Campbell M, Bougherara H, Martin MN, Yahia L'H. Biomimetic polymer composites for orthopedic implants. 2005; Boston, USA ASM International.
20. Bougherara H, Klika V, Maršík F, Bureau M N, Yahia L'H Biomimetic hip prosthesis including bone remodeling process induced by dynamical loading. In: Middleton J, editor; 2006; Antibes, Cote d'Azur, France
21. Campbell M, Bureau MN, Bougherara HA, Denault J, Yahia L'H Biomimetic HA-coated composite hip implants and cell adhesion. 2006; Charlotte, USA. In: Proceedings of the Annual Technical Conference ANTEC (SPE). p 158-162.
22. Auclair-Daigle C, Bureau MN, Legoux J-G, Yahia L'H. Bioactive Hydroxyapatite Coatings on Polymer Composites for Orthopedic Implants. Journal of Biomedical Materials Research A 2005;73A(4):398-408.
23. Bryan W, McCaskill BL, Tullos HS. Hip endoprosthesis stabilization with a porous low-modulus stem coating: factors influencing stabilization. Clin Orthop 1981;157:125-32.
24. Tullos H, McCaskill BL, Dickey R, Davidson J. Total hip arthroplasty with a low-modulus porous-coated femoral componen. J Bone Joint Surg. Am. 1984;66:888-98.
25. Spector M, Heylogers I, Roberson JR. Porous polymers for biological fixation. Clin Orthop Relat Res. 1988;235:207-19.
26. Spector M, Roberson JR, de Andrade JR. Bone growth into porous polysulfone. J. Orthop. Surg. Tech. 1987;3 21-33.
27. Adam F, Pfautsch S, Westermann K. Early failure of a press-fit carbon fiber hip prosthesis with a smooth surface. The Journal of Arthroplasty 2002;17(2):217–223.
28. Harvey E, Bobyn JD, Tanzer M, Stackpool GJ, Krygier JJ, Hacking SA. Effect of lexibility of the femoral stem on bone-remodeling and fixation of the stem in a canine total hip arthroplasty model without cement. J. Bone Joint Surg. Am. 1999;81:93-107.
29. McAuley J, Engh CA Jr. Femoral fixation in the face of considerable bone loss: cylindrical and extensively coated femoral components. Clin Orthop Relat Res 2004 429:215-21.
30. Karrholm J, Anderberg C, Snorrason F, Thanner J, Langeland N, Malchau H, Herberts P. Evaluation of a femoral stem with reduced stiffness. A randomized study with use of radiostereometry and bone densitometry. J Bone Joint Surg Am. 2002;84:1651-1658
31. Glassman AH CR, Schenck R, Herberts P. A low stiffness. composite biologically fixed prosthesis. Clin Orthop Relat Res 2001;393:128-36.
32. Akhavan S, Matthiesen MM, Schulte L, T Penoyar, Kraay M J, RimnacCM, Goldberg VM Clinical and histologic results related to a low-modulus composite total hip replacement stem. J. Bone Joint Surg. Am. 2006;88:1308-1314.

33. Weinans H, Huiskes R, Grootenboer H J. The behavior of adaptive bone-remodeling simulation models. J. Biomechanics 1992;25:1425-41.
34. Carter D, Orr TE, Fyhrie DP. Relationships between loading history and femoral cancellous bone architecture. J. Biomechanics 1989;22:231-44.
35. Weinans H, Sumner DR, Igloria R, Natarajan R N Sensitivity of periprosthetic stress-shielding to load and the bone density-modulus relationship in subject-specific finite element models. Journal of Biomechanics 2000;33(7):809-817.
36. Goldstein S, Matthews LS, Kuhn JL, Hollister SJ. Trabecular bone remodeling: an experimental model. Journal of Biomechanics 1991;24:135-150.
37. Fyhrie D, Carter DR. Prediction of cancellous bone apparent density with 3D stress analysis. Transactions 32nd Annual Orthopaedic Research Society 1986b:P331.
38. Papini M, Zalzal P Thirdgen.zip, from the International Society of Biomechanics (ISB) Finite Element Mesh Repository, Istituti Ortopedici Rizzoli. Available from: http://www.cineca.it/hosted/LTM-IOR/back2net/ISB_mesh/isb_mesh.html.
39. Balle F. Biomechanische Untersuchungen zur Knochen-Implantat-Interaktion mit Hilfe der Methode der Finiten Elemente: University of Kaiserslautern, LTM, U04-01; 2004.
40. Tompson I, Hench LL Mechanical properties of bioactive glasses, glass-ceramics and composites. Proceedings of the Institution of Mechanical Engineers. Part H, Journal of engineering in medicine 1998;212(2):127-136.
41. Rezwana K, Chena QZ, Blakera JJ, Boccaccini, AR. Biodegradable and bioactive porous polymer/inorganic composite scaffolds for bone tissue engineering. Biomaterials 2006;27(18):3413-3431.
42. Bergmann G, Graichen F, Rohlmann A. Hip joint loading during walking and running, measured in two patients. J. Biomech. 1993;27(8):969-990.
43. Terrier A, Rakotomanana RL, Ramaniraka AN, Leyvraz FP Adaptation model for anisotropic bone. Computer methods in biomechanics and biomedical engineering 1997;1(1):47-59.
44. Cristofoloni L. A critical analysis of stress shielding evaluation of hip prosthesis. Critical Reviews™ in Biomedical Engineering 1997;25(4&5):409-483.
45. Li C, Granger C, Del Schutte H, Biggers SB, Kennedy JM, Latour RA Progressive failure analysisnext term of laminated previous termcomposite femoralnext term prostheses previous termfornext term total previous termhip arthroplasty. Biomaterials 2002;23(21): 4249-4262.
46. Li C, Granger C, Del Schutte H, Biggers SB, Kennedy JM, Latour RA Failure analysis of composite femoral components for hip arthroplasty. Journal of Rehabilitation Research and Development 2003;40(2):131-146.
47. Kerner J, Huiskes R, Van Lenthe GH, Weinans H, van Rietbergen B, Engh CA, Amis AA. Correlation between pre-operative periprosthetic bone density and post-operative bone loss in THA can be explained by strain-adaptive remodelling. Journal of Biomechanics 1999;32(7):695-703.
48. Otani T, Whiteside LA, White SE Strain distribution in the proximal femur with flexible composite and metallic femoral components under axial and torsional loads. Journal of Biomedical Materials Research 1993;27(5):575-585.

49. Van Rietbergen B, Huiskes R, Weinans H, Sumner DR, Turner TM, Galante JO. The mechanism of bone remodeling and resorption around press-fitted THA stems. Journal of Biomechanics 1993;26(4-5):369-382.
50. Akay M, Aslan N Numerical and experimental stress analysis of polymeric composite hip joint prosthesis. Journal of Biomedical Materials Research 1996;31:167-182.
51. Yildiz H, Chang FK, Goodman S Composite hip prosthesis design. II. Simulation. J Biomed Mater Res 1998;39:102-119.
52. Yildiz H, Chang FK, Goodman S Composite hip prosthesis design. I. Analysis. J Biomed Mater Res 1998;39:92-101.
53. Taylor M, Tanner KE, Freeman MAR, Yetram AL Cancellous bone stresses surrounding the femoral component of a hip prosthesis: an elastic-plastic finite element analysis. Medical Engineering & Physics 1995;17:544-550.
54. Klika V, Maršík F, Bougherara H, Mařík I, Yahia L'H. Bone remodelling induced by dynamic loading - biochemical model and numerical simulation. Musculoskeletal review 2006 – Touch Briefings publication 2006.

TABLE I

Values of parameters used in Weinans et al. model[33]

Parameter	Unit	Value
B	$(g/cm^3)^2/(MPa.\ time\ unit)$	1
k	J/g	0.004
E	MPa	$3790\rho^3$
s	-----	0.35
ρ_{min}	g/cm^3	0.01
ρ_{max}	g/cm^3	1.74

154x97mm (300 x 300 DPI)

TABLE II
Mechanical properties of the composite prosthesis

Material	Modulus of Elasticity (MPa)	Shear Modulus (MPa)	Poisson's Ratio
CF/PA12 composite (± 45°)	$E_x = 15\ 400$ $E_y = 15\ 400$ $E_z = 3\ 500$	$G_{xy} = 3\ 000$ $G_{xz} = 3\ 500$ $G_{yz} = 3\ 200$	$\nu_{xy} = 0.3$ $\nu_{xz} = 0.25$ $\nu_{yz} = 0.2$
Polymeric core	$E = 600$	$G = 250$	$\nu = 0.2$

192x74mm (300 x 300 DPI)

TABLE III
Values of the Components of Hip Joint Forces Used in the FE Models

Load Case	Activity	Resultant load (N)	Load Components (N)		
			F_x	F_y	F_z
1	Single limb stance	3409	-1492	-915	2925
2	Walking	3231	-1283	-700	2882
3	Stair climbing	2318	-1034	-906	1866

188x76mm (300 x 300 DPI)

TABLE IV
Values of the Components of Muscle Forces due to Various Activities

Activity	Resultant Load (N)	Load Components (N)		
		F_x	F_y	F_z
Single Limb stance	2592	1342	832	- 2055
Walking	1086	471	144	- 967
Stair Climbing	750	375	377	- 532

200x97mm (300 x 300 DPI)

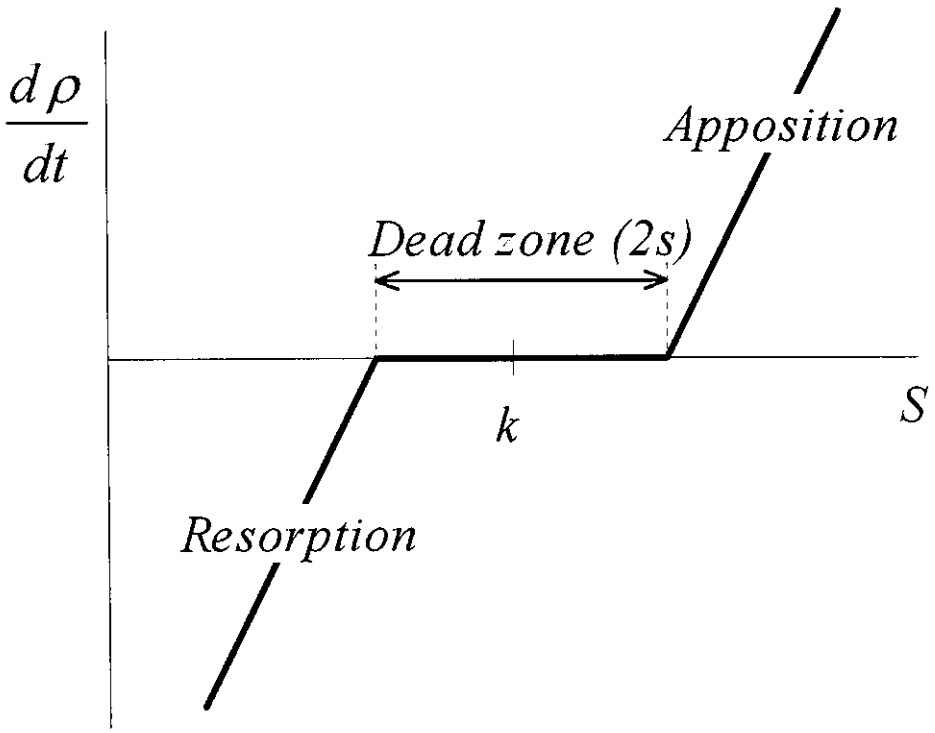

106x82mm (300 x 300 DPI)

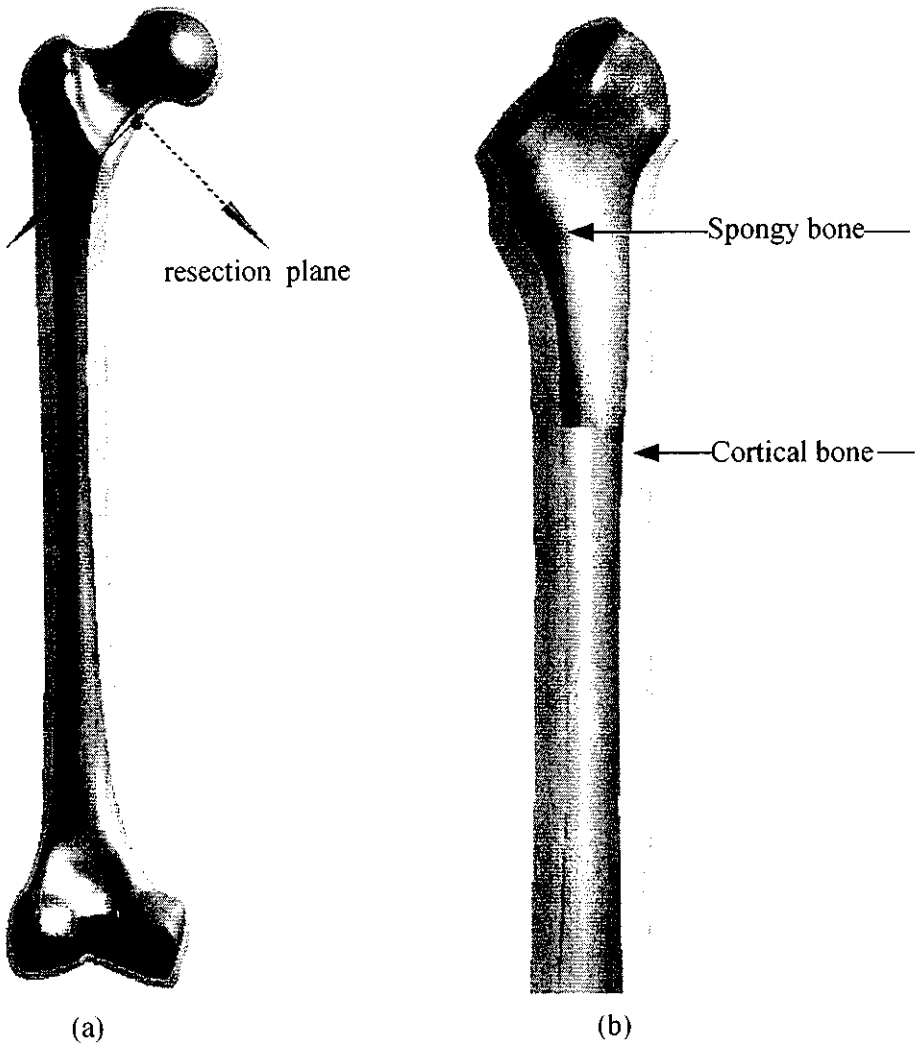

181x200mm (300 x 300 DPI)

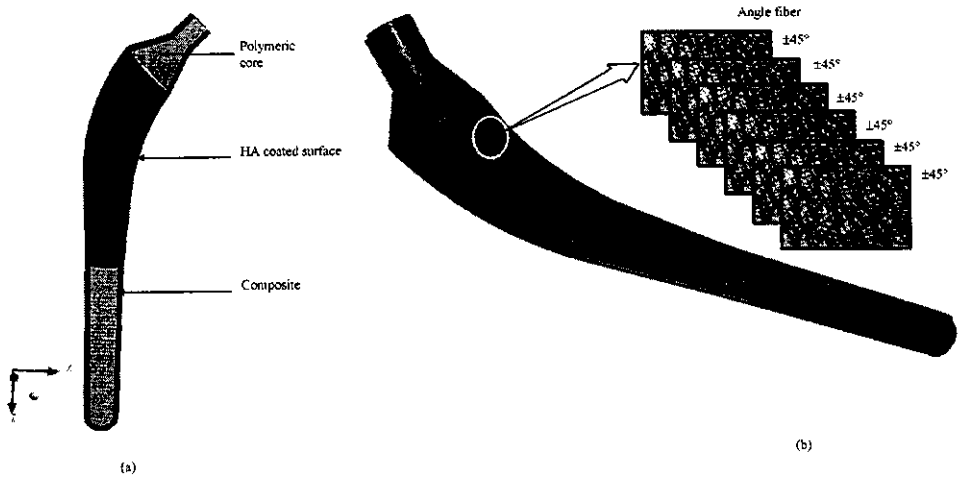

294x148mm (300 x 300 DPI)

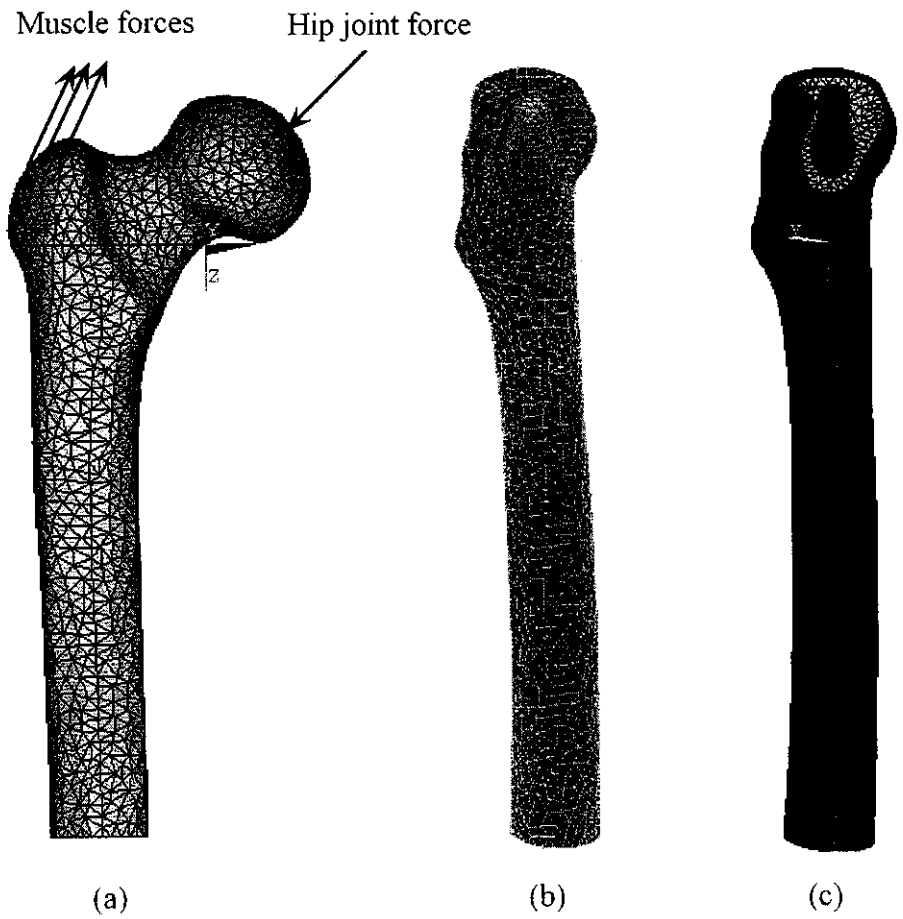

148x141mm (300 x 300 DPI)

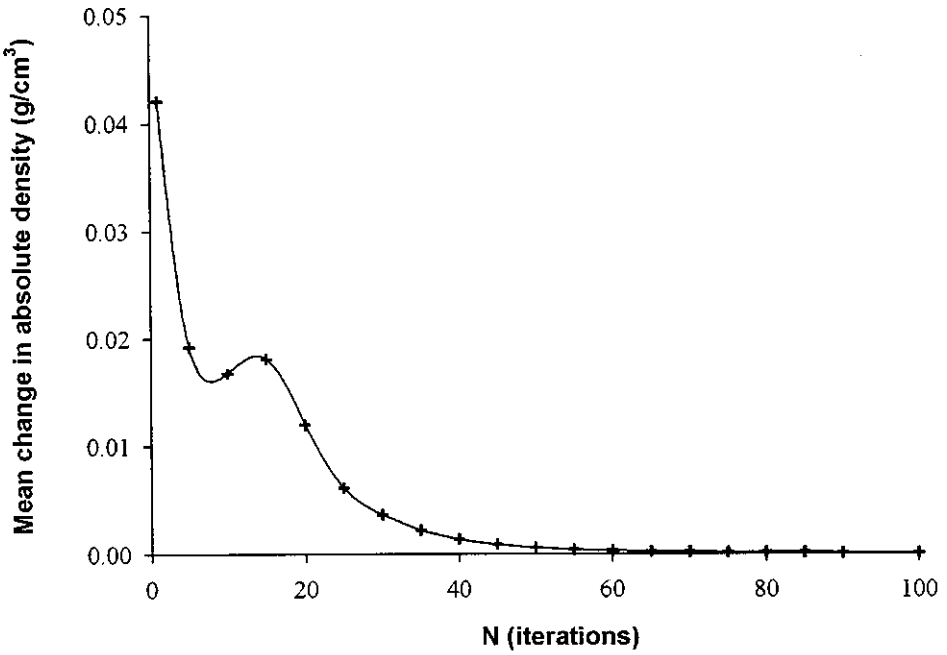

158x118mm (300 x 300 DPI)

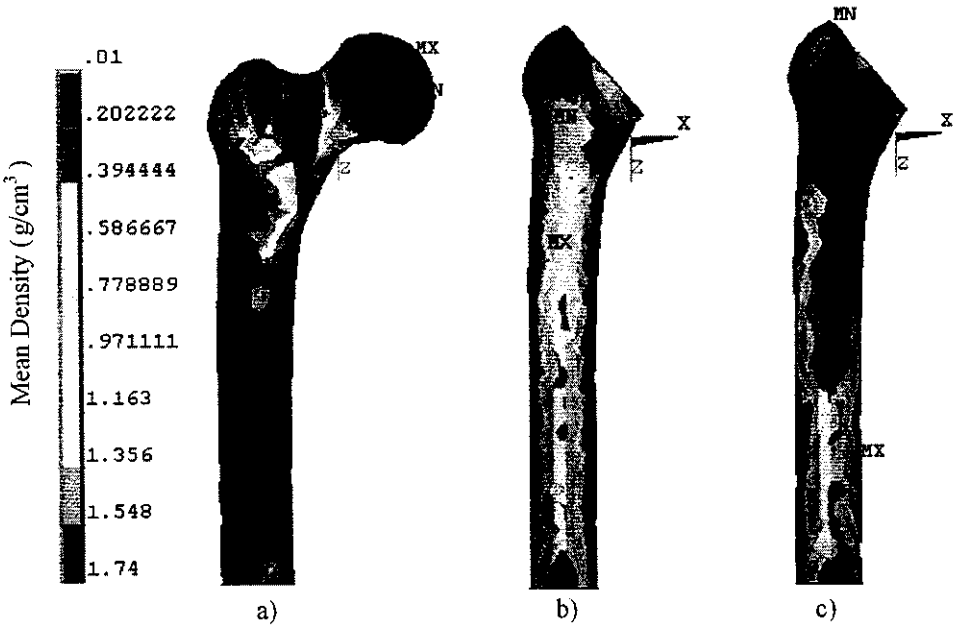

176x115mm (300 x 300 DPI)

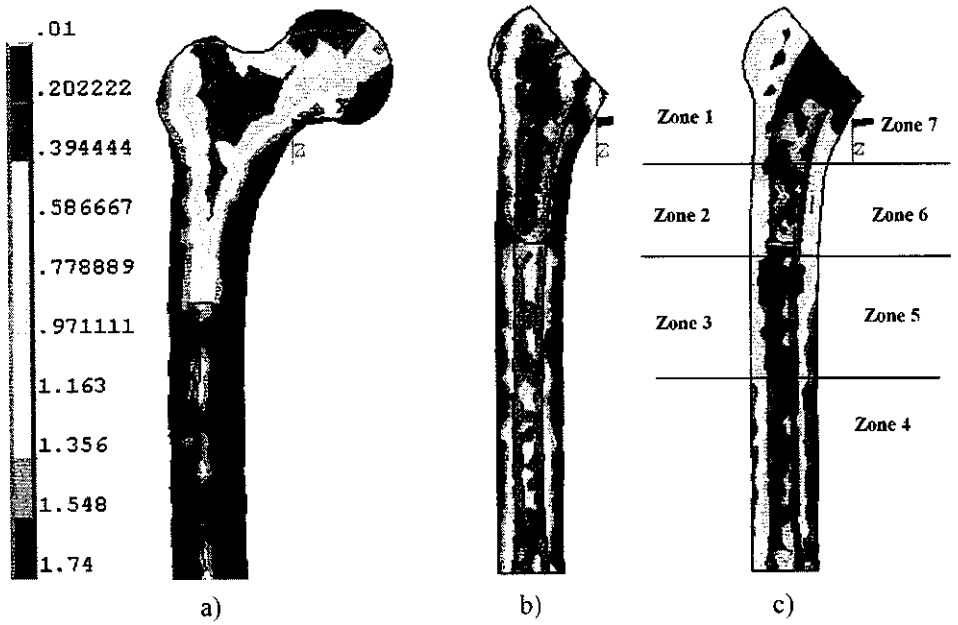

173x112mm (300 x 300 DPI)

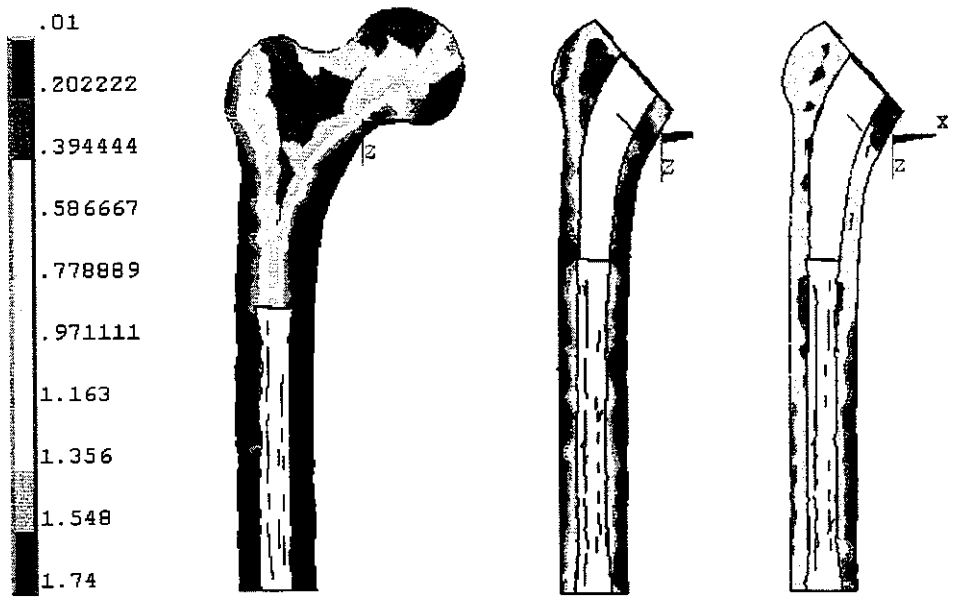

a) b) c)

157x112mm (300 x 300 DPI)

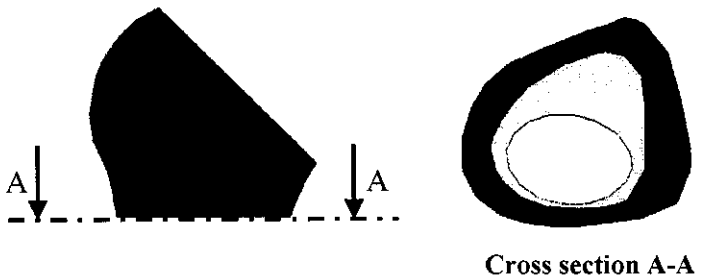

(a)

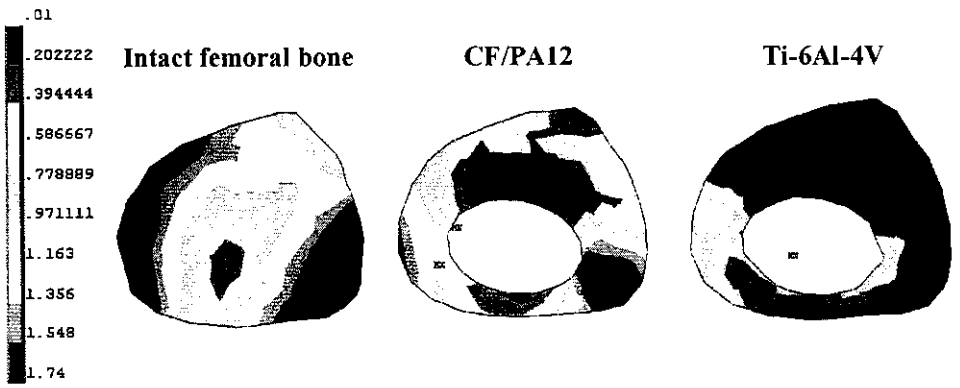

(b)

199x173mm (300 x 300 DPI)

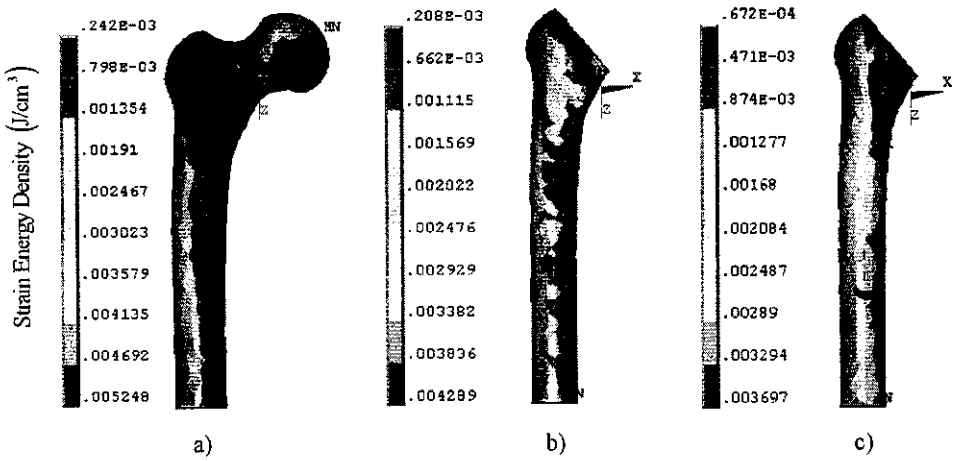

a) b) c)

194x94mm (300 x 300 DPI)

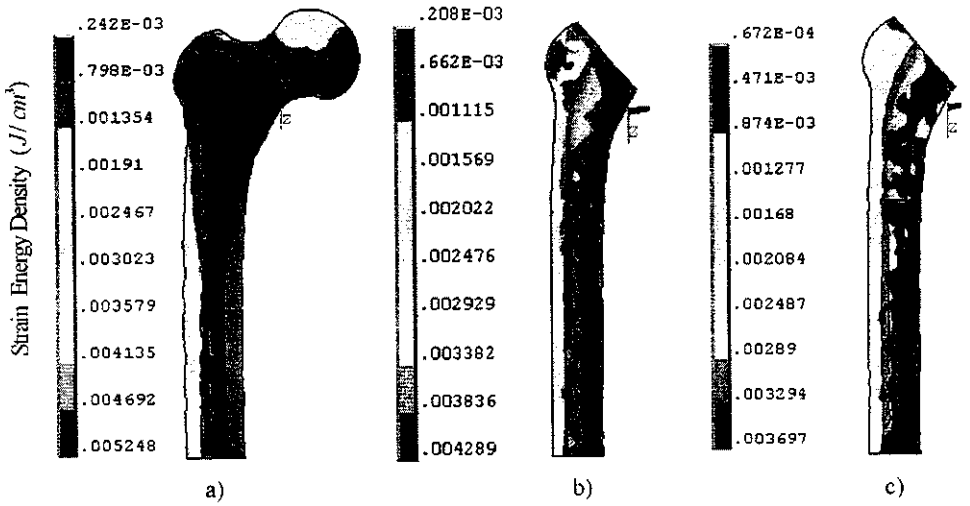

195x101mm (300 x 300 DPI)

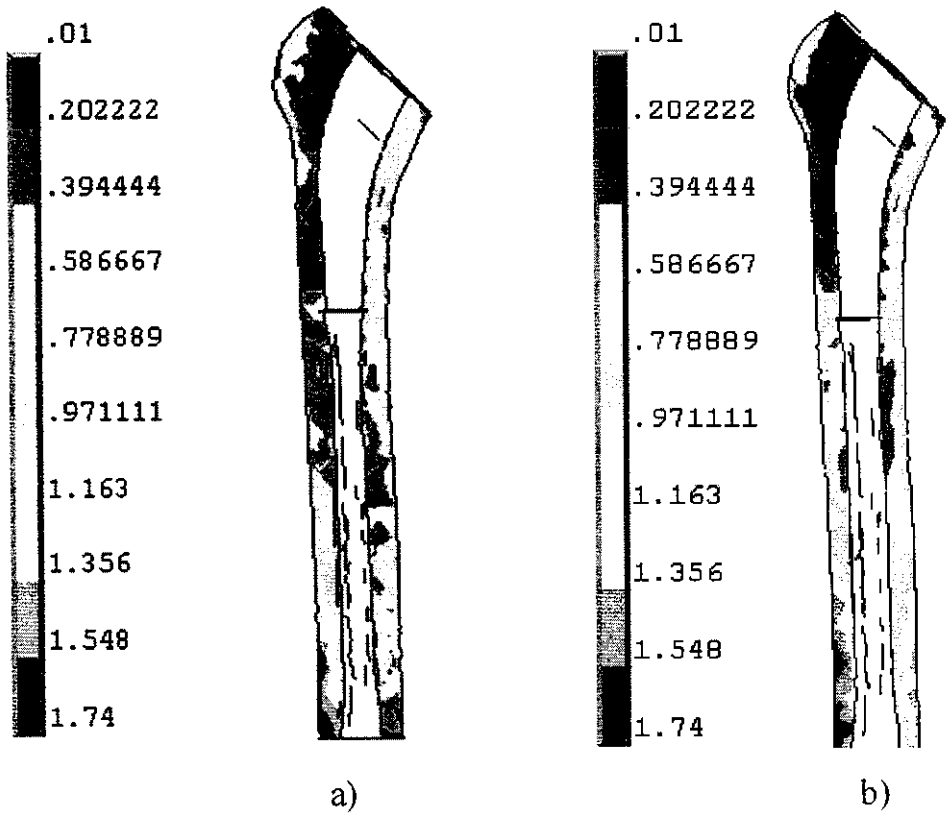

172x146mm (300 x 300 DPI)

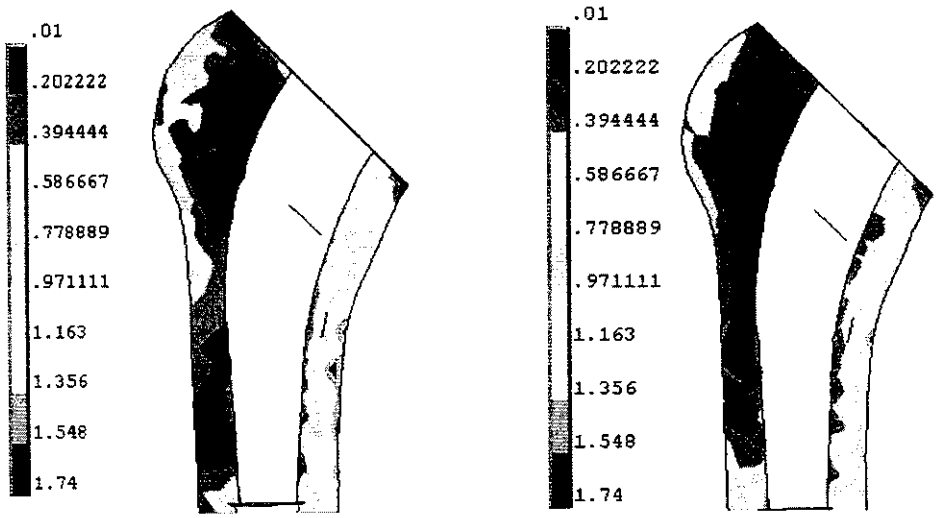

a) b)

153x92mm (300 x 300 DPI)